INFECTION AND IMMUNITY, Sept. 2007, p. 4373–4385 Vol. 75, No. 9
0019-9567/07/$08.00+0 doi:10.1128/IAI.00497-07

Transcriptional Regulation of the Heme Binding Protein Gene Family of *Bartonella quintana* Is Accomplished by a Novel Promoter Element and Iron Response Regulator▽†

James M. Battisti, Laura S. Smitherman, Kate N. Sappington, Nermi L. Parrow, Rahul Raghavan, and Michael F. Minnick*

Division of Biological Sciences, The University of Montana, Missoula, Montana 59812

Received 6 April 2007/Accepted 8 June 2007

We previously identified a five-member family of hemin-binding proteins (Hbp's) of *Bartonella quintana* that bind hemin on the outer surface but share no homology with known bacterial heme receptors. Subsequently, we demonstrated that expression of the *hbp* family is significantly influenced by oxygen, heme, and temperature conditions encountered by the pathogen in the human host and the body louse vector; e.g., we observed a dramatic (>100-fold) increase in *hbpC* transcript levels in response to the "louse-like" temperature of 30°C. The goal of the present study was to identify a transcription factor(s) involved in the coordinated and differential regulation of the *hbp* family. First, we used quantitative real-time PCR (qRT-PCR) to show that the same environmental conditions generate parallels in the transcript profiles of four candidate transcriptional regulators (Irr, Fur, RirA, and BatR) described in the order *Rhizobiales*, with the greatest overall change in the transcription of *irr* (a >5-fold decrease) at a "louse-like" temperature, suggesting that Irr may function as an *hbpC* repressor. Second, a *B. quintana* strain hyperexpressing Irr was constructed; it exhibits a "bloodstream-like" *hbp* transcript profile in the absence of an environmental stimulus (i.e., *hbpC* is repressed and *hbpA*, *hbpD*, and *hbpE* mRNAs are relatively abundant). Furthermore, when this strain is grown at a "louse-like" temperature, an inversion of the transcript profile occurs, where derepression of *hbpC* and repression of *hbpA*, *hbpD*, and *hbpE* are readily evident, strongly suggesting that Irr and temperature influence *hbp* family expression. Third, electrophoretic mobility shift analyses show that recombinant Irr binds specifically to the *hbpC* promoter region at a sequence that is highly conserved in *Bartonella hbp* genes, which we designated the *hbp* family box, or "H-box." Fourth, we used the H-box to search the *B. quintana* genome and discovered a number of intriguing open reading frames, e.g., five members of a six-member family of cohemolysin autotransporters. Finally, qRT-PCR data regarding the effects of Fur and RirA overexpression on the *hbp* family are provided; they show that Fur's effect on the *hbp* family is relatively minor but RirA generates a "bloodstream-like" *hbp* transcript profile in the absence of an environmental stimulus, as observed for the Irr-hyperexpressing strain.

The *Bartonellaceae* are members of the order *Rhizobiales*, a group of *Alphaproteobacteria* responsible for a variety of mammalian (bartonellosis, brucellosis) and plant (crown gall) diseases. *Bartonella quintana* infection of humans results in an acute febrile syndrome called trench fever, and chronic manifestations of persistent infection include endocarditis, bacillary angiomatosis, and bacillary peliosis (29, 40). *B. quintana* has affected millions of people during war and is presently re-emerging in inner cities and in AIDS patients throughout the world (11, 20, 37, 48). Although the majority of human diseases caused by the *Rhizobiales* are considered zoonoses, maintenance of *B. quintana* in nature is thought to be restricted to humans and body lice (*Pediculus humanus corporis*). Humans are infected when body louse fecal matter, or a crushed louse containing the bacterium, is introduced into the bloodstream through breaches in the integument concurrent with the itching caused by louse infestation. Overcrowded, unhygienic conditions disseminate infected lice and can quickly result in an epidemic.

Living between the clothing and skin, body lice normally take several blood meals per day and acquire *B. quintana* by imbibing the blood of a bacteremic human (12). To generate disease, *B. quintana* must survive and proliferate throughout the human-louse-human cycle and must respond to the disparate environments of the human and body louse. An environmental change of particular interest is the concentration of heme, which is used as a prosthetic subunit in a large number of proteins and consists of an iron atom contained in the center of porphyrin. (The Fe^{3+} oxidation product of heme is called hemin.) Free heme is quite rare in humans (5), whereas potentially toxic levels are generated in the louse gut during blood meals (26, 49, 65), which can occur several times daily (12). *B. quintana* has the greatest known bacterial requirement for exogenous heme (42, 43, 67), and it is generally accepted that this extraordinary supplement is needed by all members of the *Bartonellaceae*, because erythrocytes, hemoglobin, or hemin (20 to 40 μg/ml of medium) is essential for in vitro cultivation (8). Since combinations of iron and porphyrin cannot substitute for heme in cultivation, researchers have hypothesized that high levels are necessary for one or more of the following: a source of iron (14, 59) or porphyrin (43), a hydro-

* Corresponding author. Mailing address: Division of Biological Sciences, The University of Montana, Missoula, MT 59812. Phone: (406) 243-5792. Fax: (406) 243-4184. E-mail: mike.minnick@mso.umt.edu.

† Supplemental material for this article may be found at http://iai.asm.org/.

▽ Published ahead of print on 18 June 2007.

gen peroxide-detoxifying agent (42), or a means to establish a microaerobic intracellular environment (7) (as leghemoglobin functions for nitrogen-fixing rhizobia [2]). Considering the fluctuations in heme levels throughout the human-louse-human cycle and the extraordinary concentration required, it is obvious that heme acquisition mechanisms are essential for the replication and ultimately the pathogenesis of *B. quintana*.

Previously, we discovered a family of hemin-binding proteins (HbpA to HbpE) synthesized by *B. quintana* that serve as outer membrane hemin receptors yet share no similarity to known bacterial heme binding proteins (14, 41). Hbp orthologues are found throughout the *Rhizobiales*. In fact, the *Brucella* outer membrane protein (*omp*) family (16, 58, 68) has become a major focus of vaccine development (10, 22, 27), and recently it was demonstrated that Omp31 is also a hemin-binding protein (17). The obvious similarity between the *Bartonella hbp* family and the *Brucella omp* family was the impetus for the inclusion of *batR* transcript analysis in the present study (see below), since BvrR (the *Brucella* orthologue) has been implicated in the regulation of *Brucella abortus* Omp25 synthesis (23, 61). Orthologues of Hbp's are termed Rop's in the rhizobia and have been identified and partially characterized (18, 54, 55). Finally, the prediction of a beta-barrel porin-like structure for Hbp's (as well as its orthologues) suggests that Hbp's may function to bind heme and subsequently transport some portion of it (15, 73).

Recently (7), we showed that environmental signals that simulate oxygen, heme, and temperature conditions encountered by *B. quintana* in the human bloodstream (37°C, 5% O_2, low hemin) and the insect vector (30°C, high hemin) significantly influence the expression of the *hbp* family in a coordinated and differential manner. These environmental stimuli generated transcript profiles that were either "louse-like" (relatively high for *hbpC* and *hbpB* [subgroup I] and low for *hbpA*, *hbpD*, and *hbpE*) or "bloodstream-like" (relatively high for *hbpA*, *hbpD*, and *hbpE* [subgroup II] and apparently repressed for *hbpC* and *hbpB*). The most dramatic change in the transcript profile of the *hbp* family occurred in response to a "louse-like" temperature of 30°C (34, 39), where a >100-fold increase in the *hbpC* mRNA transcript level was demonstrated relative to the level at the human bloodstream temperature (37°C). We proposed that subgroup I (HbpC and, to a lesser extent, HbpB) is preferentially synthesized in the louse and that subgroup II proteins (HbpA, HbpD, and HbpE) are employed for heme acquisition in humans. Accordingly, it was recently shown that HbpE is a dominant immunoreactive surface antigen in humans infected with *B. quintana* (9). Finally, we demonstrated the existence of a *cis*-acting regulatory element located in the *hbpA* promoter region (7). The goal of the present study was to elucidate the coordinated and differential regulation of the *hbp* family, with a focus on identification of a transcriptional regulator responsible for the apparent repression of *hbpC* observed at 37°C compared to 30°C (>100-fold increase).

MATERIALS AND METHODS

Bacterial strains and culture conditions. Bacterial strains used in this study are described in Table 1. *B. quintana* strain JK31 is a low-passage virulent human isolate and was a generous gift from Jane Koehler (University of California at San Francisco). HIB plates were used to cultivate *B. quintana* in all experiments except when hemin concentrations were modified, for which *Brucella* agar-hemin was employed. HIB consists of a heart infusion broth (Becton Dickinson, Sparks, MD) base containing 1.5% Difco agar (Becton Dickinson), supplemented with 2% (vol/vol) sheep serum and 4% (vol/vol) defibrinated sheep blood (Quad Five, Ryegate, MT). *Brucella* agar-hemin consists of a *Brucella* broth (Becton Dickinson) base containing 1.5% Difco agar and supplemented with hemin chloride (Calbiochem, San Diego, CA). Hemin chloride (referred to below as hemin) was dissolved in 0.02 N NaOH to a final concentration of 5 mg/ml and was sterilized by autoclaving. Hemin was added to autoclaved *Brucella* agar to three final concentrations, 0.05 mM (low), 0.15 mM (normal), and 2.5 mM (high), as previously described (7). Chloramphenicol (Fisher Scientific, Fair Lawn, NJ) was added to a final concentration of 1 μg/ml for the selection and propagation of pBBR1MCS-containing plasmids. *B. quintana* was routinely grown at 37°C in a humidified 5% CO_2 incubator. The growth temperature was modified by cultivation in a humidified 5% CO_2 incubator at 30°C. The O_2 concentration of the cultivation environment was lowered from 21% to 5% by replacing atmospheric air in a Pyrex vacuum desiccator jar (Corning, St. Louis, MO) with a blood-gas mixture (5% CO_2, 5% O2, 90% N_2; NorLab, Boise, ID) as previously described (7). Approximately 96 h was required for *Bartonella* to reach mid-log phase regardless of growth conditions or hemin supplementation.

Escherichia coli strains TOP10F′, DH5α, and M15(pREP4), employed in cloning experiments, were cultivated using Luria-Bertani medium with standard concentrations of antibiotic supplements (4) when required.

Nucleic acid isolation, purification, and manipulation. The plasmids used in this study are described in Table 1. For primers, see Table S1 in the supplemental material. Standard restriction endonucleases, PCR, and cloning procedures were employed for the construction of plasmids (4). The Perfectprep Plasmid Mini kit (Eppendorf, Hamburg, Germany) and the QIAquick spin kit (QIAGEN, Valencia, CA) were used for plasmid isolation and DNA purification, respectively, during routine cloning procedures. Plasmids employed in electroporation were

TABLE 1. Bacterial strains and plasmids

Strain or plasmid	Relevant characteristic	Source or reference
Strains		
B. quintana		
JK31	Low-passage virulent human isolate	J. Koehler
JK31+pBBR	JK31 with pBBR1MCS	This study
JK31+pBBR-IRR	JK31 with pBBR-IRR	This study
JK31+pBBR-FUR	JK31 with pBBR-FUR	This study
JK31+pBBR-RIRA	JK31 with pBBR-RIRA	This study
E. coli		
TOP10F′	Host strain for cloning	Invitrogen
DH5α	Host strain for cloning	Gibco-BRL
M15(pREP4)	Host strain for His_6 fusion protein rIrr	Qiagen
Plasmids		
pCR2.1TOPO	TA cloning vector	Invitrogen
pCR2.1TOPO-IRR	pCR2.1TOPO containing *B. quintana irr*	This study
pCR2.1TOPO-RIRA	pCR2.1TOPO containing *B. quintana rirA*	This study
pCR2.1TOPO-FUR	pCR2.1TOPO containing *B. quintana fur*	This study
pBBR1MCS	Shuttle vector for *Bartonella*	31
pBBR1MCS-IRR	pBBR1MCS containing *B. quintana irr*	This study
pBBR1MCS-RIRA	pBBR1MCS containing *B. quintana rirA*	This study
pBBR1MCS-FUR	pBBR1MCS containing *B. quintana fur*	This study
pQE30	Expression vector for His_6 fusion proteins	Qiagen
pQE-IRR	*B. quintana* recombinant Irr expression plasmid	This study

prepared using the Wizard Midiprep kit (Promega, Madison, WI). *Bartonella* genomic DNA was prepared with the DNeasy tissue kit (QIAGEN) for the PCR template. Primers for PCR and sequence analysis were synthesized by Sigma-Genosys (The Woodlands, TX). Nucleic acids were quantified by using a Spectronic Genesys 2 spectrophotometer (Milton Roy, Rochester, NY).

B. quintana mRNA used for quantitative real-time PCR (qRT-PCR) and transcriptional start site (TSS) mapping was prepared using the RiboPure-Bacteria kit with Turbo DNase I treatment (Ambion, Austin, TX) and a FastPrep bead homogenizer (Qbiogene, Carlsbad, CA) according to the manufacturers' instructions. The primers and probes used for qRT-PCR analysis of the *hbp* family have been described previously (41). The *irr*, *rirA*, and *fur* primer-probe sets, as well as the *batR* primer set, used for qRT-PCR analysis were designed with Beacon Designer, version 4.0 (Bio-Rad, Hercules, CA) and are listed in Table S1 in the supplemental material. Dual-labeled *irr*, *rirA*, and *fur* probes were synthesized with fluorescent tags as described for the *hbp* family (41); 5-carboxyfluorescein and *N*,*N*′,*N*′-tetramethyl-6-carboxyrhodamine were covalently linked to the 5′ and 3′ ends, respectively (Sigma-Genosys). The *irr*, *rirA*, *fur*, and *batR* primer pairs were synthesized by Applied Biosystems (ABI; Foster City, CA).

qRT-PCR. qRT-PCR using RNAs derived from bacteria subjected to altered growth environments (hemin, O_2, or temperature) or from genetically modified bacteria (containing multiple copies of a specific transcription factor) was used to calculate the "fold difference," defined as the amount of a specific target mRNA normalized to an endogenous reference and relative to a calibrator. For example, the amount of a specific transcriptional regulator (*irr*, *rirA*, *fur*, or *batR*) mRNA in 30°C preparations (target) was normalized to the amount of 16S rRNA (endogenous reference) and is relative to the quantity of that particular transcriptional regulator mRNA in the 37°C preparations (calibrator). Specifically, *hbp*, *irr*, *rirA*, and *fur* qRT-PCR results were obtained using One-Step RT-PCR Master Mix, MultiScribe, and RNase inhibitor reagents (ABI) with the MyiQ Real-Time PCR detection system (Bio-Rad) and Optical System software, version 1.0 (Bio-Rad), as previously described (7). Each reaction mixture included 0.7 ng template RNA, 67 ng probe, and 167 ng of each primer in a 25-μl volume and a 96-well format. Cycling parameters were 50°C for 30 min, 95°C for 10 min, and then 40 cycles of 95°C for 15 s and 60°C for 60 s. Fold differences in transcript levels were calculated by using the comparative cycle threshold method (3, 33). Because our laboratory is transitioning to the use of more cost-effective RT-PCR reagents, *batR* qRT-PCR results were obtained by using the iScript One-Step RT-PCR kit with SYBR green (Bio-Rad) per the manufacturer's instructions. Protocols and equipment were the same as those described above, except that the reaction conditions were 50°C for 10 min, 95°C for 5 min, and then 40 cycles of 95°C for 15 s and 60°C for 30 s. Three independent determinations of fold differences were used to calculate the average fold difference values and associated standard deviations reported here.

Construction of *irr*, *fur*, and *rirA* overexpression plasmids. Primers were designed to generate *irr*, *fur*, and *rirA* PCR amplicons from *B. quintana* that contained the open reading frame (ORF) as well as flanking sequence. (i) The *irr* amplicon is 782 bp with 181 bp upstream and 99 bp downstream of the ORF; (ii) the *fur* amplicon is 533 bp with 82 bp of upstream and 53 bp of downstream flanking sequence; and (iii) the *rirA* amplicon is 740 bp with 185 bp of upstream sequence and 107 bp downstream of the ORF (see Table S1 in the supplemental material). Amplicons were cloned into pCR2.1TOPO, resulting in pCR2.1TOPO-IRR, pCR2.1TOPO-FUR, and pCR2.1TOPO-RIRA. Each target ORF and specified flanking sequence was cloned into pBBR1MCS. (i) The KpnI/XbaI fragment from pCR2.1TOPO-IRR was cloned into KpnI/XbaI-digested pBBR1MCS, resulting in pBBR-IRR; (ii) the XbaI/HindIII fragment from pCR2.1TOPO-FUR was cloned into XbaI/HindIII-digested pBBR1MCS, resulting in pBBR-FUR; and (iii) the KpnI/XbaI fragment from pCR2.1TOPO-RIRA was cloned into KpnI/XbaI-digested pBBR1MCS, resulting in pBBR-RIRA. Plasmid contents were verified by sequence analysis.

Transformation of *B. quintana*. pBBR1MCS overexpression constructs were introduced into *B. quintana* by electroporation as previously described (6, 7). Briefly, strain JK31 (in vitro passages 5 to 8) was harvested into heart infusion broth, washed in 10% glycerol, and diluted to 3×10^{10} cells/ml with 10% glycerol. A 44-μl volume of bacteria was combined with 5 μl of plasmid DNA (~3 μg/μl) in a 2-mm-gap electroporation cuvette (BTX, Holliston, MA) and pulsed with a GenePulser (Bio-Rad) at 2.5 kV, 25 μF, and 400 Ω. Several chloramphenicol-resistant clones were further examined and verified as stable transformants by restriction fragment length polymorphism (RFLP) analysis of plasmid preparations.

Cloning, expression, and purification of rIrr. Primers were designed (see Table S1 in the supplemental material) to generate a 500-bp amplicon that contained the *irr* ORF, which was subsequently cloned into pCR2.1TOPO. The HindIII/PstI fragment from this plasmid was then cloned into compatible sites of pQE30, resulting in pQE30-IRR. Following transformation of *E. coli* M15(pRep4), induction and purification of His_6-tagged recombinant Irr (rIrr) (under native conditions) were accomplished using the manufacturer's protocols (QIAGEN).

EMSA analysis. Electrophoretic mobility shift assay (EMSA) analysis was accomplished with the LightShift chemiluminescent EMSA kit (Pierce, Rockford, IL) according to the manufacturer's instructions. Initially, four overlapping PCR products specific to the *hbpC* promoter region were generated with primer pairs listed in Table S1 in the supplemental material and *B. quintana* JK31 genomic DNA. Amplicons were then biotinylated with the biotin 3′ end DNA labeling kit (Pierce) according to the manufacturer's instructions, and these biotinylated amplicons are referred to as "probes" below. EMSA reaction mixtures were prepared as follows: 10× binding buffer (2 μl), 50% glycerol (1 μl), 1-μg/μl poly(dI-dC) (1 μl), 1% NP-40 (1 μl), and 40 fmol of a biotin-labeled probe. rIrr alone (1.4 μM) or in combination with an unlabeled probe (8 pmol) was added, and the final volume was brought to 20 μl with distilled H_2O. Following a 20-min incubation at room temperature, reaction mixtures were loaded onto a 5% nondenaturing polyacrylamide gel and electrophoretically separated at 4°C using 0.5% Tris-borate-EDTA buffer. The biotinylated probes were then transferred at 4°C to Immobilon-NY^+ membranes (Millipore, Bedford, MA) by using 0.5% Tris-borate-EDTA and a Mini Trans-Blot cell (Bio-Rad) and were cross-linked by a 15-min exposure on a UV transilluminator. Finally, biotinylated probes were visualized using a chemiluminescent nucleic acid detection module (Pierce) according to the manufacturer's instructions.

Determination of TSSs of *hbp* genes and *irr*. TSSs were analyzed using primer extension (PE) and random amplification of cDNA ends (RACE). Total RNA for TSS mapping was isolated from *B. quintana* (96-h cultures) with a RiboPure-Bacteria kit according to the manufacturer's instructions (Ambion). To analyze TSSs by PE, HBP-PE primers (see Table S1 in the supplemental material) (10 pmol) were end labeled using [γ-^{32}P]ATP (New England Nuclear, Boston, MA) and T4 polynucleotide kinase as instructed by the supplier (Promega). Labeled primers were annealed to 100 μg RNA in hybridization buffer [40 mM piperazine-*N*,*N*′-bis(2-ethanesulfonic acid) (PIPES; pH 6.4), 1 mM EDTA, 0.4 M NaCl, 80% formamide] for 16 h at 50°C. The resulting hybrid was precipitated with 95% ethanol and the pellet dried in vacuo. PE was carried out using Moloney murine leukemia virus reverse transcriptase and a supplied buffer containing deoxynucleoside triphosphates and RNasin according to the manufacturer's instructions (Promega). Extension products were loaded onto a sequencing gel adjacent to DNA sequencing reactions generated with a Sequenase 2.0 kit (U.S. Biochemicals, Cleveland, OH) using the same TSS primer, a plasmid DNA template containing the respective *hbp* gene plus flanking sequences cloned into pBluescript SK (41), and α-^{35}S-labeled dATP (New England Nuclear). To analyze TSSs by RACE, the 5′ RACE system (Invitrogen-Life Technologies, Carlsbad, CA) was used according to the manufacturer's instructions along with GSP1 and GSP2 primers specific to each target (see Table S1 in the supplemental material). cDNAs of each target transcript were synthesized using a GSP1 primer and Superscript II reverse transcriptase. Following addition of a 3′ dC tail to the cDNA, a nested GSP2 primer and the 5′ Abridged Anchor Primer were used to PCR amplify the target cDNA. The amplicons were cloned into pCR2.1TOPO, and plasmid preparations of *E. coli* TOP10 transformants were sequenced in both strands.

Nucleotide sequencing and analysis. DNA was sequenced with an automated DNA sequencer (ABI 3130x1) and a BigDye Terminator cycle sequencing ready reaction kit (ABI). Sequence analysis was accomplished with MacVector software, version 9.0 (Accelrys, San Diego, CA). Genomic DNA sequences of *B. quintana* strain Toulouse (NC_005955), *Bartonella henselae* strain Houston-1 (NC_005956) (1), and *Bartonella bacilliformis* strain KC583 (NC_008783) were obtained from the National Center for Biotechnology Information (http://www.ncbi.nlm.nih.gov).

RESULTS

Environmental stimuli generate parallels within transcription factor qRT-PCR patterns. Previously, we reported a correlation between biologically significant environmental cues and differential expression of the *hbp* family (7), and the largest overall fold difference in any of the *hbp* transcripts occurred in response to a "louse-like" temperature, where a dramatic increase in *hbpC* levels (>100-fold) was observed. In the present study, we were interested in identifying transcription

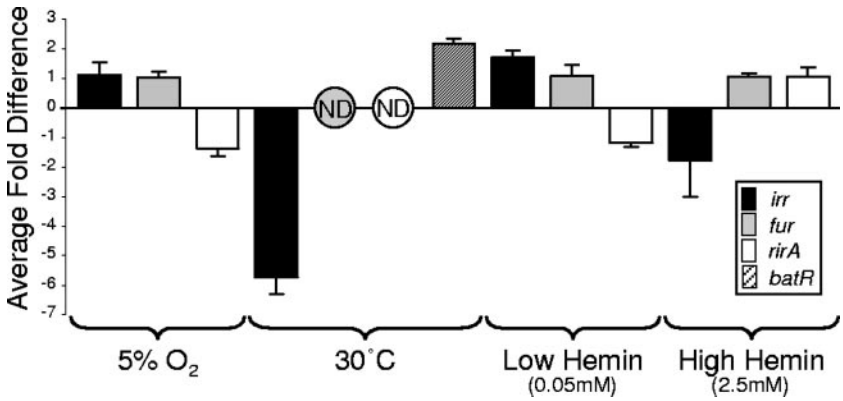

FIG. 1. Environmental stimuli generate parallels within transcriptional regulator mRNAs. Shown are average fold differences in the mRNA quantities of transcriptional regulators *irr*, *fur*, *rirA*, and *batR*, relative to the quantities from the control environment (21% O_2, 37°C, 0.15 mM hemin), following growth under conditions that simulate the oxygen, temperature, and heme conditions of the host and vector. At 96 h, the amount of transcription factor mRNA from each environment (5% O_2, 30°C, low or high hemin) was normalized to the amount of 16S rRNA. Error bars represent standard deviations from three independent triplicate determinations. ND, not detectable, i.e., the average cycle threshold value is statistically indistinguishable from that for the no-template control.

factors involved in regulation of the *hbp* family. Thus, we used qRT-PCR to determine if heme- or iron-related transcription factors (*irr*, *fur*, *rirA*, or *batR*) were influenced by the same "louse-like" (30°C, high hemin) or human "bloodstream-like" (5% O_2, low hemin) conditions. The protocols and compound calculations of the comparative method of qRT-PCR (3) determine fold difference. The average fold difference reported in this study is the average of three independent fold difference calculations (done in triplicate), with associated standard deviations. Transcript profiles for the temperature comparison, as well as for O_2 (5% for the target; 21% for the calibrator) and hemin (0.05 mM or 2.5 mM for the target; 0.15 mM for the calibrator), are shown in Fig. 1.

First, it is apparent that the transcript profiles resulting from independent "bloodstream-like" or "louse-like" cues generate similar responses: (i) both "bloodstream-like" stimuli (5% O_2 and low hemin) generate profiles where *irr* and *fur* mRNA quantities are slightly elevated and that of *rirA* is slightly reduced, and (ii) both "louse-like" stimuli (30°C and high hemin) produce reductions in *irr* transcript levels. A similar parallel response to these "louse-like" and "bloodstream-like" stimuli previously resulted in a division of the *hbp* family into two subgroups (subgroup I comprises *hbpC* and *hbpB*; subgroup II comprises *hbpA*, *hbpD*, and *hbpE*) (7). Collectively, these environmentally induced parallels in expression suggest that one or more of these iron- or heme-related transcriptional regulators are involved in differential and coordinated expression of the *hbp* family. Second, the "louse-like" stimulus of a lower growth temperature generated a differential transcript profile for *fur* and *rirA*, where neither transcript ($n = 9$ for each) was detectable at 30°C, yet a slight increase was apparent in RNA preparations from *B. quintana* grown under high hemin conditions. Previously, temperature was hypothesized to be the major environmental cue responsible for differential expression of the *hbp* family, and corroborating evidence is provided below. Third, the quantity of the *batR* transcript was determined on the 30°C preparation to demonstrate the overall inverse relationship between *irr* and *batR* evident throughout our results. (A unique exception to this trend is evident in Fig. 2B at a "louse-like" temperature.) Finally, the largest overall average fold difference was observed in response to a "louse-like" temperature, where a >5-fold decrease in *irr* levels is apparent at 30°C compared to 37°C. The inverse relationship between *irr* and *hbpC* suggests that Irr may be an *hbpC* transcriptional repressor.

Temperature and Irr influence *hbp* family transcript profiles. We further investigated the relationship between *irr* and the *hbp* family by using qRT-PCR with a combination of temperature stimuli and a genetically engineered strain, *B. quintana* strain JK31+pBBR-IRR. Initially, pBBR-IRR, containing the *irr* ORF and flanking sequence, was constructed. Following transformation of *B. quintana* JK31, chloramphenicol-resistant clones were screened, and one of these, JK31+pBBR-IRR, was verified by plasmid preparations and RFLP analysis to maintain pBBR-IRR as an autonomously replicating plasmid. The calibrator strain, JK31+pBBR, was transformed, selected, and verified by identical methods.

Average fold differences were calculated for *hbpA* to *hbpE*, *irr*, *fur*, *rirA*, and *batR* from RNA preparations of JK31+pBBR-IRR (target) and JK31+pBBR (calibrator) cultivated in a control environment (HIB, 37°C, 21% O_2). The results of this experiment are shown in Fig. 2A. Multiple copies of *irr* and flanking sequence generate interesting profiles for both the *hbp* family and the transcriptional regulators. First, it is obvious that the presence of multiple copies of *irr* (with an endogenous promoter) leads to a marked increase (>380-fold) in the quantity of *irr* mRNA and is likely a result of the copy number of pBBR1MCS. A commensurate difference in the level of Irr protein between these two strains was confirmed by immunoblot analysis using rabbit anti-Irr antiserum (data not shown), showing that JK31+pBBR-IRR is, in effect, an Irr-hyperexpressing (hyper-Irr) strain. Second, we previously hypothesized that expression of subgroup I (*hbpC* and *hbpB*) was "louse specific," because these transcripts predominated following "louse-like" stimuli (30°C, high hemin), and that subgroup II expression was "human specific," because "bloodstream-like" stimuli (37°C, low hemin) resulted in significant increases in *hbpA*, *hbpD*, and *hbpE* levels (7). The subgroup I

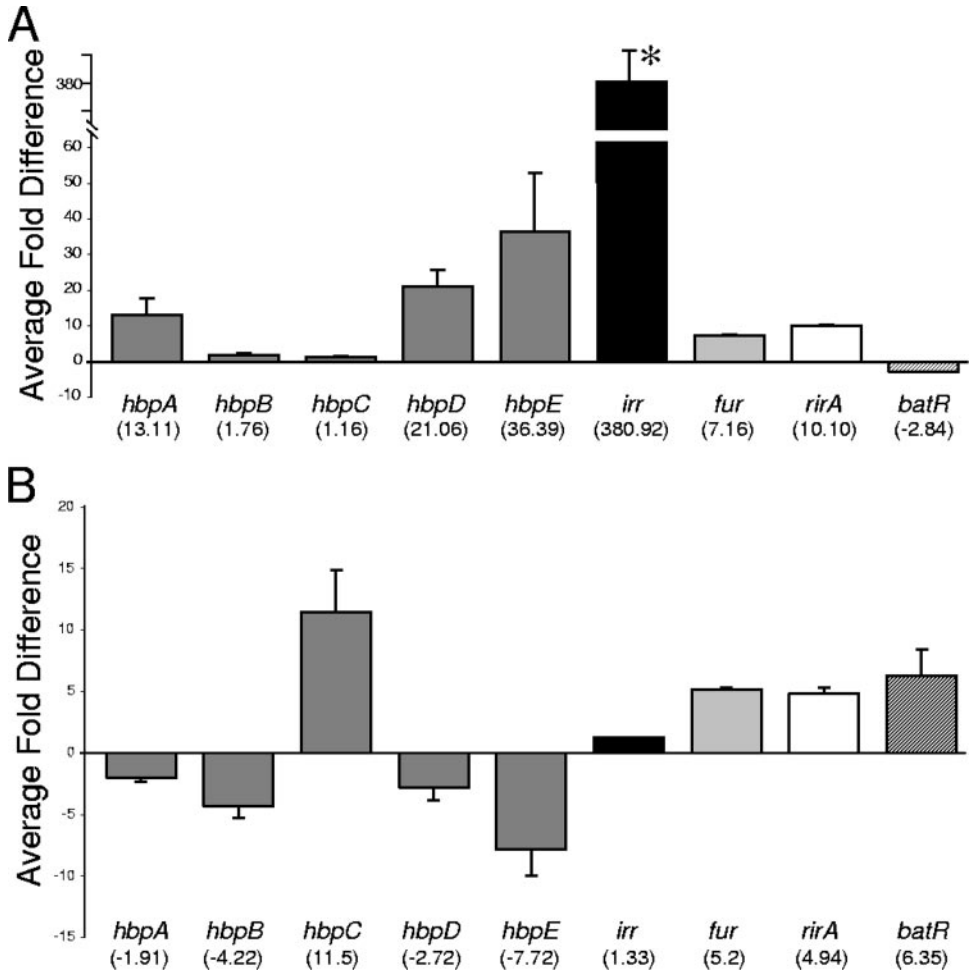

FIG. 2. qRT-PCR analysis of a hyper-Irr strain at 37°C and 30°C. Shown are average fold differences observed at 37°C (A) and 30°C (B) between the mRNA quantities of *hbp* genes and transcription factors *irr*, *fur*, *rirA*, and *batR* from a hyper-Irr strain (JK31+pBBR-IRR) and those from a control strain (JK31+pBBR). At 96 h, the amount of target mRNA from JK31+pBBR-IRR was normalized to the amount of 16S rRNA. Error bars represent standard deviations from three independent triplicate determinations. The asterisk indicates that the error bar is not drawn to scale.

repression exhibited by the hyper-Irr strain, combined with the substantial increase in subgroup II expression, is analogous to a "bloodstream-like" *hbp* family transcript profile under normal growth conditions (Fig. 2A). Collectively, these data suggest that Irr plays a role in regulating the *hbp* family. Lastly, levels of *rirA* transcripts exhibit the largest overall fold change among the remaining transcriptional regulators, followed by *fur* and *batR* in this strain.

Since the hyper-Irr strain exhibits a "human-specific" *hbp* family transcript profile in a control environment, we set out to learn more about the relationship between Irr and *hbp* expression by studying the effects of a "louse-like" stimulus on JK31+pBBR-IRR. The response of wild-type *B. quintana* JK31 to a "louse-like" temperature was a dramatic (>100-fold) increase in *hbpC* transcript levels (7) and a >5-fold decrease in *irr* levels, as demonstrated here (Fig. 1). These changes constitute the largest overall fold difference seen for any *hbp* and for all transcriptional regulators tested. Therefore, if Irr is involved in *hbpC* repression, we would best observe this event at 30°C. Average fold differences were calculated for *hbpA* to *hbpE*, *irr*, *fur*, *rirA*, and *batR* from RNA preparations of JK31+pBBR-IRR grown at a "louse-like" temperature (HIB, 30°C, 21% O_2) (target) compared to the control environment (HIB, 37°C, 21% O_2) (calibrator) and are shown in Fig. 2B. First, the insignificant change in the *irr* transcript quantity (1.33) implies that the hyper-Irr phenotype is maintained at 30°C. Second, in comparison to the >100-fold increase in *hbpC* levels observed for wild-type *B. quintana* at 30°C (7), the hyper-Irr strain generates only a small increase in *hbpC* transcript levels at 30°C (Fig. 2B), yet it is not fully repressed, as demonstrated at 37°C (Fig. 2A). These data show that Irr and temperature have significant and inversely related effects on *hbpC* transcription; *hbpC* expression is seemingly repressed by Irr and is greatly enhanced at 30°C. Third, the hyper-Irr strain exhibits a noteworthy reduction in *hbpA*, *hbpD*, and *hbpE* transcript quantities at a "louse-like" temperature (Fig. 2B) compared to growth at 37°C (Fig. 2A) or wild-type expression at 30°C (7). This suggests that expression of *hbp* subgroup II is also influenced by temperature and Irr; *hbpA*, *hbpD*, and *hbpE* are up-regulated in the presence of Irr and are repressed at

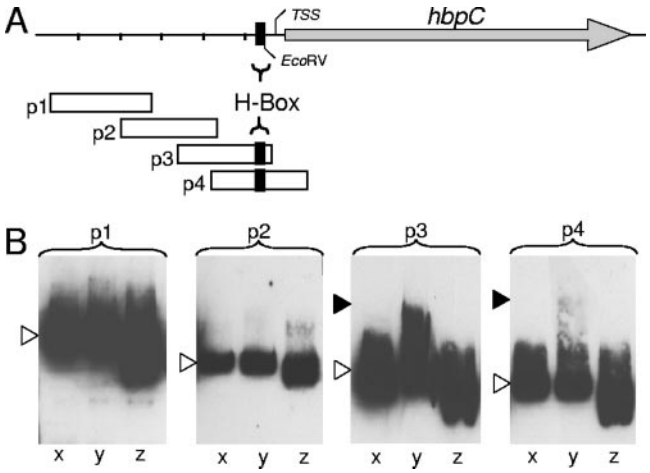

FIG. 3. rIrr EMSA of the *hbpC* promoter region. (A) Diagram of the *hbpC* promoter and relevant characteristics. The locations of biotin-labeled probes (p1, p2, p3, p4) used for EMSA are indicated, as are the relative locations of the H-box, the *hbpC* TSS, and the EcoRV restriction site that eliminates the rIrr-specific shift. Tick marks are placed every 100 bp. (B) Comparison of the mobilities of the four *hbpC* promoter probes (40 fmol) alone (lanes x), in the presence of 1.4 μM rIrr (lanes y), and combined with 1.4 μM rIrr and 8 pmol of an unlabeled probe (lanes z). Solid arrowheads indicate shifted probes; open arrowheads indicate the normal migratory position.

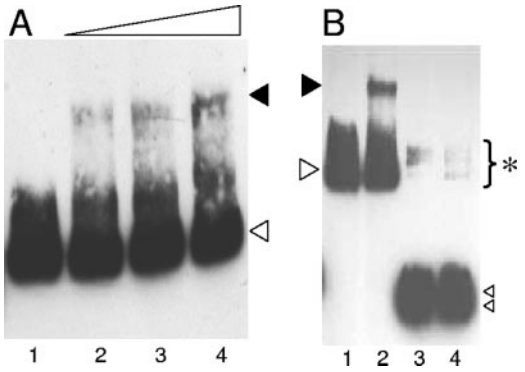

FIG. 4. EMSA of *hbpC* probe 4 demonstrates the specificity and location of the rIrr *cis*-acting element. (A) An increase in the intensity of the EMSA shift of *hbpC* probe 4 (40 fmol) (lane 1) is apparent upon addition of increasing amounts of rIrr—1.4 μM (lane 2), 2.0 μM (lane 3), and 3.0 μM (lane 4)—demonstrating the specificity of binding. (B) Comparison of the mobility of *hbpC* probe 4 (lanes 1 and 2) to the mobility of the two nearly equal sized EcoRV fragments of probe 4 (lanes 3 and 4). A mobility shift is apparent when 40 fmol of probe 4 alone (lane 1) is combined with 1.4 μM rIrr (lane 2), yet neither of the probe 4 EcoRV fragments (lane 3) demonstrates a shift when combined with 1.4 μM rIrr (lane 4), indicating that the rIrr *cis*-acting element is in close proximity to the EcoRV site. Solid arrowheads mark shifted probe 4, and open arrowheads point to the normal migratory position of probe 4, or probe 4 fragments (double open arrowhead). The asterisk indicates residual undigested probe 4, which is present in equal amounts in lanes 3 and 4, and not a mobility shift.

30°C. Taken together, it appears as if the hyper-Irr strain augments the effect of the temperature stimulus on *hbp* expression. Last, although changes observed in the remaining transcriptional regulators are not as extreme, two points are worth mentioning: (i) neither *rirA* nor *fur* transcripts were detectable in wild-type *B. quintana* at 30°C (Fig. 1), yet these transcripts are relatively abundant in the hyper-Irr strain at both temperatures (Fig. 2), implying that Irr plays a role in their expression; and (ii) *batR* transcript levels have thus far been observed to increase only at a "louse-like" temperature, and as with the *hbp* genes, the hyper-Irr strain appears to augment the 30°C response (Fig. 2B) compared to that for the wild type (Fig. 1).

EMSA demonstrates binding of rIrr to the *hbpC* promoter. The qRT-PCR data presented thus far suggest a role for Irr in (i) the differential regulation of the *hbp* family, (ii) the regulation of *fur*, *rirA*, and *batR*, and (iii) the differential response to temperature. We therefore focused on the strongest correlation revealed in these qRT-PCR results by further investigating the role of Irr in *hbpC* repression. Specifically, we wanted to determine if this repressive effect was the direct result of Irr activity at the *hbpC* promoter. Thus, four primer pairs (P1, P2, P3, and P4 [see Table S1 in the supplemental material]) were used to generate four overlapping PCR fragments (~200 bp) from the promoter region of *B. quintana* JK31 *hbpC*. Following biotinylation, these overlapping probes (p1 to p4) (Fig. 3A) were used in EMSA reactions to determine if the presence of rIrr retarded their electrophoretic migration on a polyacrylamide gel (indicating that rIrr is binding to that particular probe).

Initially, we used EMSA to analyze all four *hbpC* promoter probes. The results are shown in Fig. 3B. This EMSA method, as described in the LightShift protocol (Pierce), is designed to demonstrate two parameters of rIrr affinity for a specific *hbpC* probe. First, by comparing the mobility of the probe alone (40 fmol) (Fig. 3B, lanes x) to the migration of this probe in the presence of rIrr (1.4 μM) (lanes y), a retardation in mobility indicates that binding is occurring. Although the presence of rIrr did not alter the migration of probes 1 and 2, both probes 3 and 4 exhibited electrophoretic mobility shifts upward. The second parameter addressed in this experiment was binding specificity. If a specific binding event is occurring between rIrr and biotin-labeled probes 3 and 4, excess unlabeled probe (8 pmol) (Fig. 3B, lanes z) should competitively inhibit rIrr binding to the labeled probe and effectively eliminate the mobility shift. Elimination of the mobility shift is clearly evident in Fig. 3B, lanes z, indicating that a specific binding event is occurring between rIrr and probes 3 and 4. This also demonstrates that rIrr is binding to the *hbpC* promoter within the 158-bp region where probes 3 and 4 overlap. The slight increase in probe mobility in the presence of excess unlabeled probe (Fig. 3B, lanes z) is presumably due to the significant quantity of DNA in these reactions. Finally, EMSA reactions using lysates from the control *E. coli* strain containing pQE30 (the vector used to generate rIrr) did not produce this shift (data not shown).

To further address the specificity and location of rIrr binding within the *hbpC* promoter, we focused on probe 4 and used two common variations of EMSA described above. The results of these experiments are shown in Fig. 4. First, additional evidence regarding specificity was achieved by adding increasing amounts of rIrr to 40 fmol biotin-labeled probe 4. Compared to the biotin-labeled probe alone (Fig. 4A, lane 1), the intensity of the mobility shift is increasingly enhanced upon incremental addition of rIrr, demonstrating a specific interaction between probe 4 and rIrr. Second, we further defined the

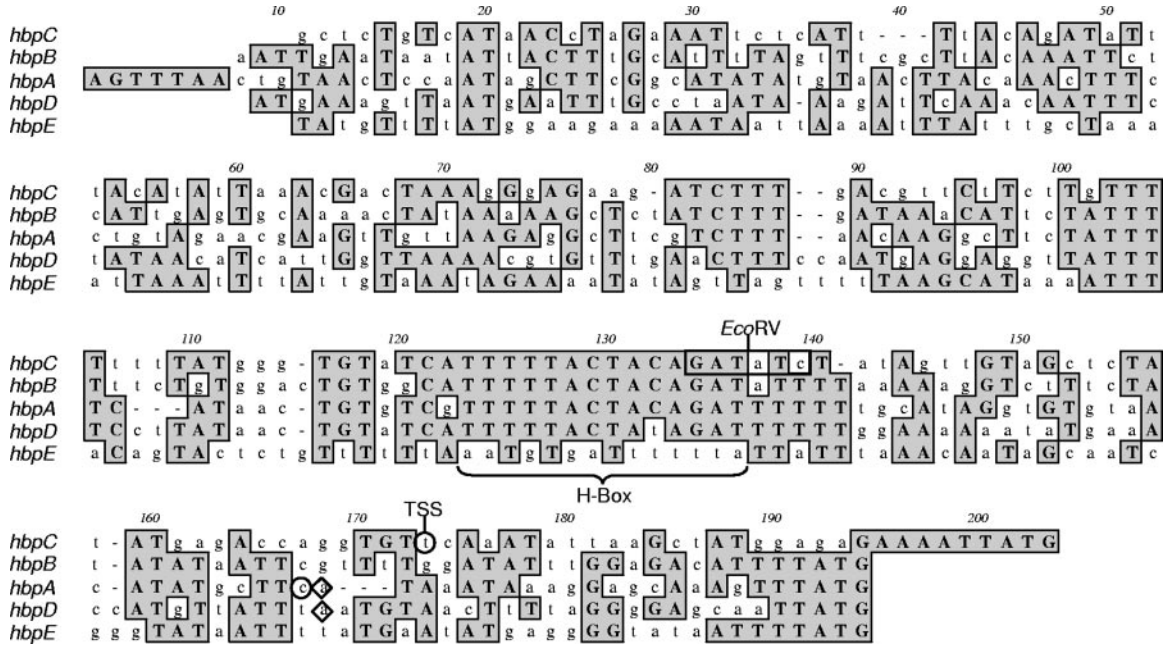

FIG. 5. Analysis of the *B. quintana hbp* family promoter. The *hbpC* promoter region from the 5′-most end of the probe 3–probe 4 overlap to the start codon of the *hbpC* ORF is shown aligned by ClustalW with the *B. quintana hbpA*, *hbpB*, *hbpD*, and *hbpE* promoter sequences (180 bp 5′ of the ATG start codon). The EcoRV site and the putative *B. quintana* Irr *cis*-acting element (H-box) are indicated. The TSSs of three *hbp* genes were mapped by PE (circles) or RACE (diamonds) and are located ~32 bp from the H-box.

location of the rIrr *cis*-acting element by EMSA analysis with EcoRV-digested probe 4. Specifically, the PCR fragment generated from primer pair P4 was restricted with EcoRV prior to purification and biotinylation. These probe 4 derivatives are of nearly equal size and comigrate during electrophoresis (Fig. 4B, lanes 3 and 4). Compared to the obvious mobility shift of probe 4 in the presence of rIrr (Fig. 4B, lane 2), neither of the EcoRV probe 4 fragments demonstrates a shift in the presence of rIrr (Fig. 4B, lane 4). This strongly suggests that the rIrr-specific *cis*-acting promoter element has been disrupted and that the motif is located in close proximity to the EcoRV site (Fig. 3A and 5).

Analysis of the *hbp* family promoter reveals the "H-box." qRT-PCR data demonstrate that Irr and temperature have a significant and differential effect on *hbp* family transcription. We hypothesized that Irr is interacting with a *cis*-acting element common to all *hbp* promoters and that some other temperature-associated modification of Irr activity is involved in differential subgroup expression. Thus, we further analyzed the *hbp* promoter regions of *B. quintana* (Fig. 5) as well as of *B. henselae* and *B. bacilliformis* (Fig. 6) to identify a potential *cis*-acting element common to all *hbp* genes. First, the *hbpC* promoter region from the 5′ end of the probe 3–probe 4 overlap sequence to the start codon of the *hbpC* ORF was

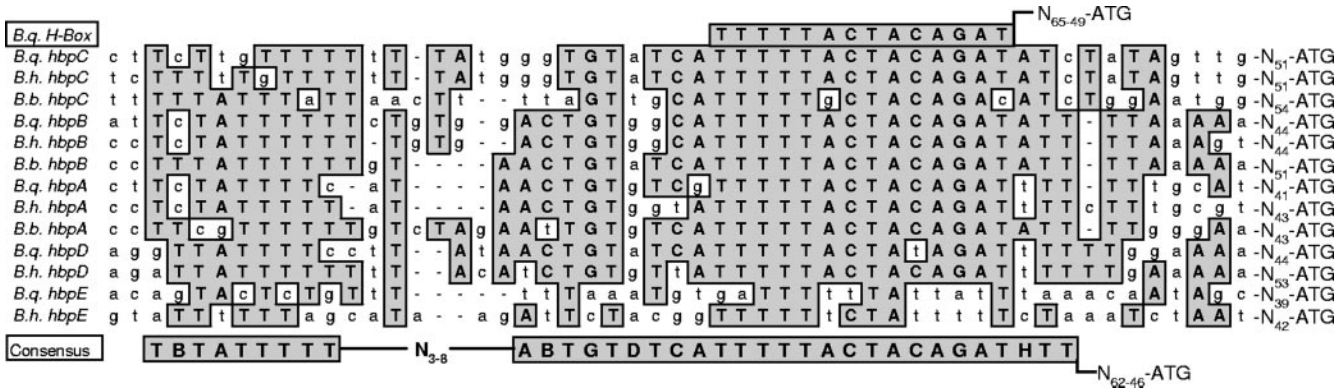

FIG. 6. Alignment of *Bartonella hbp* family promoter regions. ClustalW alignment of all *hbp* promoter region sequences (180 bp 5′ of the ATG start codon) from *B. quintana* (*B.q.*), *B. henselae* (*B.h.*), and *B. bacilliformis* (*B.b.*) demonstrates that the H-box is a highly conserved region of a larger (~40-bp) consensus shown here. Distances to the ATG codon are indicated. Note that sequences coding for *hbpD* and *hbpE* are absent in the *B. bacilliformis* genome.

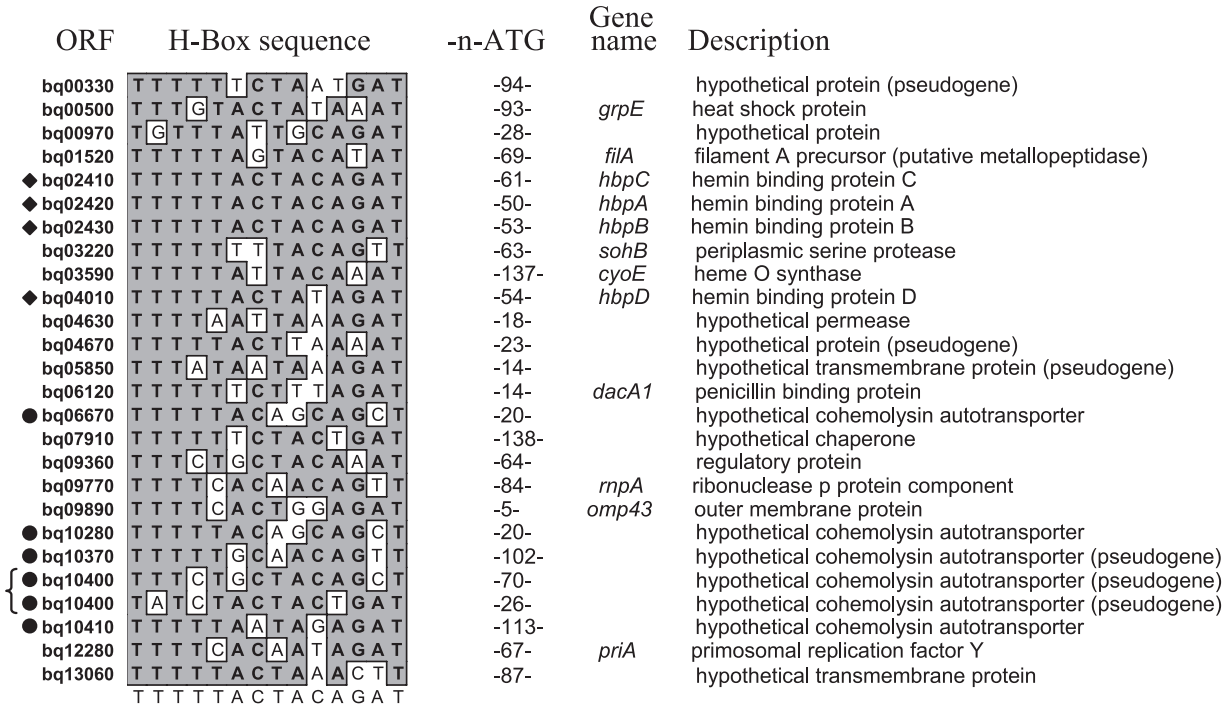

FIG. 7. Other *B. quintana* promoters contain the H-box. A search for the H-box sequence (5′-TTTTTACTACAGAT) in the *B. quintana* genome with a tolerance of 3 mismatches, within 150 bp of the predicted start codon of the indicated ORF and in the same orientation with respect to the ORF as that of the H-box relative to the *hbp* genes, identifies 26 H-box sequences. The four *hbp* genes are each marked with a diamond. The H-box also occurs in five of six members of the cohemolysin autotransporter family (solid circles), heme O synthase, and several potential virulence factors. Distance to the predicted start codon (-n-ATG), gene name, and a brief description are provided. The brace indicates two H-box sequences found in the bq10400 promoter.

aligned by ClustalW to the *B. quintana hbpA*, *hbpB*, *hbpD*, and *hbpE* promoter sequences (180 bp 5′ to the ATG start codon) (Fig. 5). The promoter sequences appear quite similar by visual inspection, and the pairwise similarity matrix data associated with this ClustalW alignment show that the *hbpC* promoter is most similar to *hbpD* (49.1% identity) and least similar to *hbpE* (36.9%) (data not shown). Second, the *B. quintana* Irr *cis*-acting element is disrupted following EcoRV digestion, and the longest (14-bp) contiguous motif shared among *hbp* genes is located immediately 5′ to the EcoRV site (the exception is *hbpE*). We further investigated this potential motif by alignment of all *hbp* promoter sequences (180 bp 5′ to the ATG start codon) from *B. quintana*, *B. henselae*, and *B. bacilliformis* and demonstrated that the sequence of this 14-bp element (5′-TTTTTACTACAGAT) and the distance to the ORF are highly conserved throughout *Bartonella hbp* genes (Fig. 6). As a result, we named this putative *cis*-acting sequence the *hbp* family box, or "H-box." In fact, the H-box appears to be a highly conserved region of a larger, ~40-bp consensus sequence that is common to all *hbp* genes. For clarification, *hbpD* and *hbpE* sequences were not found in *B. bacilliformis* and thus were not included in Fig. 6. Third, we determined that a distance of ~32 bp separates the H-boxes and TSSs of the three *hbp* genes mapped thus far (Fig. 5), suggesting that the transcriptional initiation complex is assembled in close proximity to the Irr binding site. Repeated attempts to map the *hbpB* and *hbpE* TSSs by both PE and RACE were unsuccessful. Finally, the TSS of *B. quintana irr* was mapped by RACE at two locations in the *irr* promoter (T-N_{89}-ATG and T-N_{39}-ATG), and an H-box sequence (with four mismatches) was found nearby (N_{119}-ATG), a 29-bp separation from the most distal TSS, suggesting that Irr may interact with its own promoter. Collectively, these data demonstrate a correlation between the H-box and *B. quintana* Irr that could possibly explain *hbp* regulation.

We were curious whether the H-box sequence could be used to identify other genes potentially regulated by Irr, reinforcing the significance of the motif. To this end, we searched for the H-box sequence (5′-TTTTTACTACAGAT) in the *B. quintana* genome, allowing for 3 mismatches (11 bases out of 14), and identified 417 locations (a tolerance of 4 mismatches resulted in 3,339 locations, approximately 1 site every 500 bp). We then scored these 417 sites based on distance and orientation to each ORF. Specifically, a candidate ORF was termed positive if an H-box was found in the promoter region within 150 bp upstream of the ORF and on the same strand as that on which the H-box is situated with respect to *hbp* genes. This stringent scoring method resulted in 26 total loci, listed in Fig. 7. Four of the 26 positive ORFs are *hbp* genes (*hbpA* to *hbpD*). Of the remaining 22 sites, 6 are found in the presumptive promoter regions of ORFs that are homologous to the cohemolysin family of autotransporters previously described for *B. henselae* (32). The fact that the H-box search identified an entirely different family of heme acquisition ORFs located throughout the genome suggests a common regulatory theme. Although further study is required to determine if the *B. quintana* cohemolysin family transcript profile is influenced by Irr, this in-

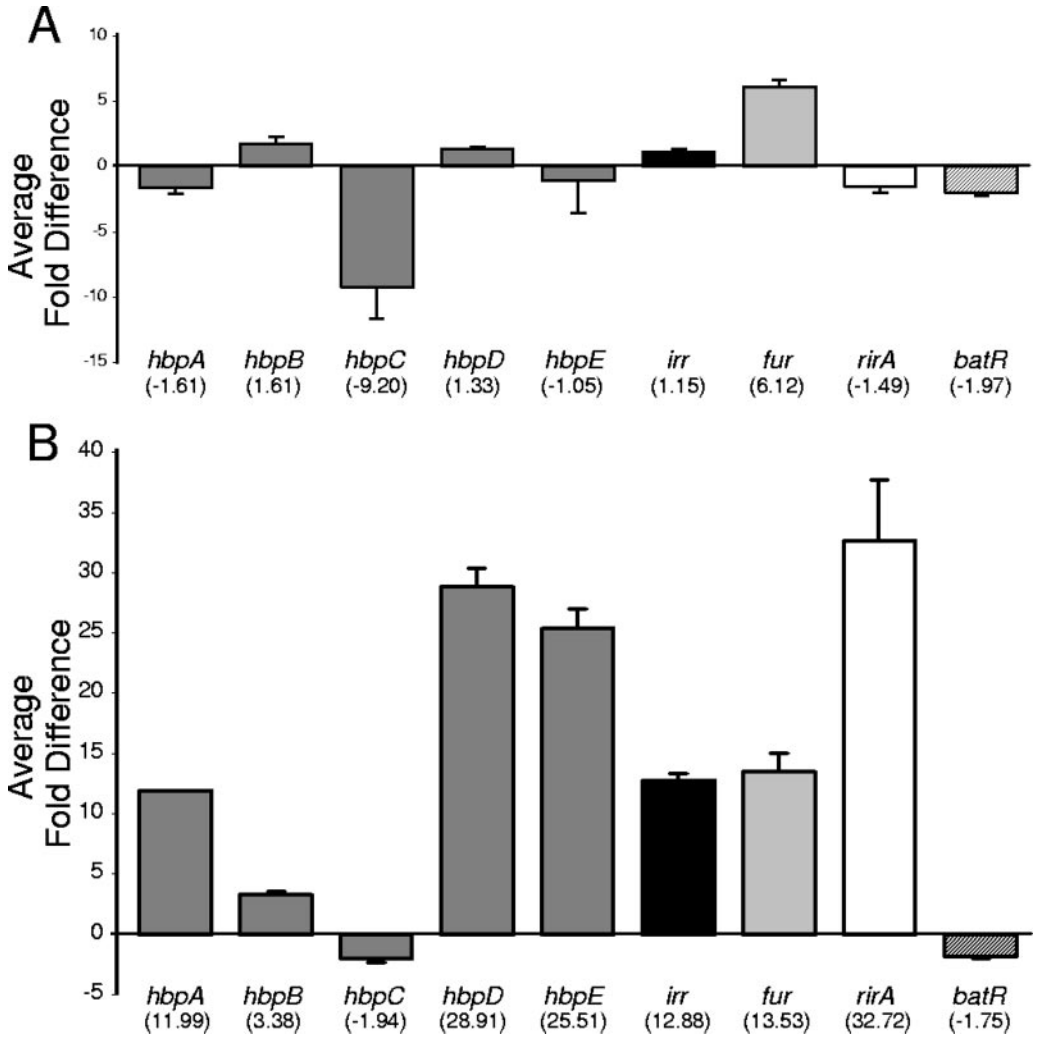

FIG. 8. qRT-PCR analysis of *B. quintana* Fur and RirA overexpression. (A) Average fold differences observed in the mRNA quantities of the *hbp* genes and *irr*, *fur*, *rirA*, and *batR* from the Fur overexpression strain (JK31+pBBR-FUR) compared to those for a control strain (JK31+pBBR). At 96 h, the amount of target mRNA from JK31+pBBR-FUR was normalized to the amount of 16S rRNA. Error bars represent standard deviations from three independent triplicate determinations. (B) Average fold differences observed in the RNA quantities of *hbp* genes and *irr*, *fur*, *rirA*, and *batR* from the *rirA* overexpression strain (JK31+pBBR-RIRA) compared to those for the control strain (JK31+pBBR). At 96, h the amount of target mRNA from JK31+pBBR-RIRA was normalized to the amount of 16S rRNA. Error bars represent standard deviations from three independent triplicate determinations.

triguing finding is discussed below. *B. quintana* is unable to synthesize heme, yet of the three heme biosynthesis ORFs that are present, *cyoE*, encoding the enzyme that converts protoheme IX to heme O, contains an H-box. This subsequence analysis of the *B. quintana* genome clearly supports the relationship between the H-box and heme-associated ORFs and implies that Irr may be involved in the regulation of these genes as well.

Response of the *hbp* family to *fur* and *rirA* overexpression. We further studied *fur* and *rirA* in relation to *hbp* family expression by using qRT-PCR and genetically engineered strains JK31+pBBR-FUR and JK31+pBBR-RIRA. Initially, plasmids pBBR-FUR and pBBR-RIRA, containing *B. quintana fur* or *rirA* with flanking sequence, were constructed (as detailed in Materials and Methods). Following transformation of low-passage *B. quintana* JK31, chloramphenicol-resistant colonies were screened and verified by plasmid preparations and RFLP analysis to maintain pBBR-FUR or pBBR-RIRA as autonomously replicating plasmids, resulting in strains JK31+pBBR-FUR and JK31+pBBR-RIRA, respectively.

First, average fold differences were calculated for *hbpA* to *hbpE*, *irr*, *fur*, *rirA*, and *batR* from RNA preparations of JK31+pBBR-FUR (target) and strain JK31+pBBR (calibrator) cultivated in a control environment (HIB, 37°C, 21% O_2). The results of this experiment are shown in Fig. 8A. Although the increase is far less than that observed for pBBR+JK31-IRR, the presence of multiple copies of *fur* and flanking sequence results in a significant increase in *fur* transcript levels. A corresponding difference in Fur protein levels between these two strains was confirmed by immunoblotting using rabbit anti-Fur antiserum (data not shown). However, changes in the quantities of all other target mRNAs were unremarkable ex-

cept for *hbpC*, where a noteworthy decrease was observed. We are downplaying the role of Fur in the regulation of *B. quintana hbp* genes for a number of reasons: (i) no parallels between *hbp* family expression and *fur* are apparent; (ii) environmental stimuli did not significantly alter the low-level transcription of *fur* throughout this study, with the exception of the "louse-like" temperature, where no *fur* transcript was detected (Fig. 1); and (iii) as discussed below, a disparity exists within the *Rhizobiales* regarding a role for Fur when RirA is present (28, 56).

Second, the average fold differences were calculated for *hbpA* to *hbpE*, *irr*, *fur*, *rirA*, and *batR* from RNAs of JK31+pBBR-RIRA (target) and strain JK31+pBBR (calibrator) cultivated in a control environment (HIB, 37°C, 21% O_2). The results of this experiment are shown in Fig. 8B. It is obvious that multiple *rirA* copies lead to a large increase (>32-fold) in *rirA* mRNA levels. The subgroup I repression exhibited by JK31+pBBR-RIRA, combined with the substantial increase in subgroup II expression, is analogous to a "bloodstream-like" *hbp* transcript profile in the absence of environmental stimuli. This *hbp* transcript profile is strikingly similar to that for the hyper-Irr strain (Fig. 2A), suggesting that both Irr and RirA play roles in *hbp* regulation. There was no obvious repressive effect on any of the other transcriptional regulator genes, although significant increases in both *irr* and *fur* are apparent. The possible direct role of RirA in *hbp* regulation is currently under investigation.

DISCUSSION

The human body louse has been implicated as the vector for three major human pathogens: *Rickettsia prowazekii* (epidemic typhus), *Borrelia recurrentis* (relapsing fever), and *B. quintana* (trench fever). Body lice live between the skin and clothing of humans (where the temperature is approximately 30°C [34, 39]) and acquire human blood meals several times daily (12), whereupon erythrocytes are hemolyzed almost immediately (65). The primary niche of *B. quintana* is the louse gut lumen (19, 26). As a result, these bacteria are exposed to waves of potentially toxic heme, iron, and reactive oxygen species with each blood meal (5, 25). The environmental conditions experienced by *B. quintana* in a human are quite different. Available heme is scavenged by hemopexin, hemoglobin, and serum albumin, and free iron is chelated by a number of molecules, depending on whether the bacterium is intracellular or extracellular. Previously (7), we reported a correlation between biologically relevant environmental cues and differential expression of the *hbp* family. In the previous study, the largest overall fold difference in any of the *hbp* transcripts occurred in response to a "louse-like" temperature, where a dramatic increase (>100-fold) was observed. It has been well documented that environmental signals induce expression of virulence determinants in bacteria (38), and it is evident that temperature is an environmental stimulus that significantly influences their expression in many vector-borne pathogens (30, 60). In this study, the largest overall fold difference for any transcriptional regulator tested was that for *irr* in response to a "louse-like" temperature of 30°C. It is intriguing that an "H-box" occurs in the promoter of the *grpE* heat shock protein (Fig. 7), and further analysis may provide interesting clues regarding the temperature-associated attributes of *hbp* regulation.

Niches occupied by bacteria are predicated on their ability to adapt to a specific environment, survive, and replicate. *Bartonella* requires a mammalian host and is typically transmitted by hematophagous insects, whereas *Rhizobium* and *Bradyrhizobium* form a symbiotic relationship with their legume host plant by fixing atmospheric nitrogen in root nodules. For nitrogen fixation to occur, a microaerobic environment must be established for the bacteria. This is accomplished by the binding of plant-generated leghemoglobin (a molecule similar to hemoglobin, the major source of heme for *Bartonella*) to the rhizobial surface, effectively shielding the bacteria, and O_2-labile nitrogenase, from oxygen (2, 46). Interestingly, the heme prosthetic group of leghemoglobin is produced by rhizobia (47), whereas in silico analysis of available bartonellae suggests that they are incapable of de novo heme synthesis, since genes for nearly all porphyrin biosynthetic enzymes are absent (7). In addition, it has been shown that a number of *Rhizobium* and *Bradyrhizobium* species can use bovine hemoglobin as an iron source, a feature thought to be restricted to animal pathogens (45), and a heme uptake system was subsequently described for *Bradyrhizobium japonicum* (44). To our knowledge, the capacity of *Bartonella* to utilize leghemoglobin in place of hemoglobin, or how the presence of these molecules influences respiration, has not been studied. The majority of studies regarding the regulation of iron- and/or heme-related genes in the *Rhizobiales* have focused on *B. japonicum* and *Rhizobium leguminosarum* and thus provided a basis for the selection of candidate transcription factors in this study (for recent reviews, see references 28 and 56). To our knowledge, the transcriptional regulation of these candidate transcription factors or Hbp orthologues has not been studied directly in conjunction with temperature and oxygen stimuli, and thus, further discussion is speculative. Furthermore, since *B. quintana* requires heme for growth, it appears impossible to differentiate a low-iron environment from a low-heme environment. If it is assumed that high-heme conditions are equivalent to high-iron conditions (and low-heme to low-iron conditions), parallel regulatory patterns are evident for *B. quintana* Irr, Fur, and RirA throughout the *Rhizobiales*.

Irr, the iron response regulator, was first identified in *B. japonicum* (24), where aberrant protoporphyrin accumulation (under iron-limited conditions) was attributed to an *irr* mutation and concurrent derepression of *hemB* (encoding the heme biosynthetic enzyme δ-aminolevulinic acid dehydratase), and is a member of the Fur (ferric uptake regulator) superfamily. Since this initial description, a number of reports have demonstrated that Irr is involved in the regulation of iron- and heme-associated genes in *B. japonicum* (44, 52, 57, 71), *R. leguminosarum* (63, 69), and *B. abortus* (35, 36). The general consensus of these studies is that (i) Irr activity is highest under iron limitation, (ii) Irr can function as a transcriptional repressor as well as an activator, (iii) heme itself can degrade Irr (51), and oxidative stress promotes degradation (70). Accordingly, we provide evidence that (i) *irr* transcript quantity is significantly increased under low-hemin (0.05 mM) conditions and is reduced under high-hemin (2.5 mM) conditions (Fig. 1); (ii) Irr can function as both a negative (*hbpC*) and a positive (*hbpA*, *hbpD*, *hbpE*) regulator (Fig. 2); and (iii) Irr has an effect on the

expression of other transcriptional regulators (Fig. 2A). Finally, the hyper-Irr strain generated an augmented "bloodstream-like" *hbp* transcript profile (Fig. 2A). Further study is required to determine if one of these other transcription factors is, along with temperature, participating in *hbp* expression. Irr is considered to be restricted to the *Rhizobiales*, and this is the first analysis of *irr* in *Bartonella*.

A *cis*-acting regulatory sequence associated with Irr function has been proposed for *B. japonicum* (44, 53, 57). First, it is worth mentioning that the original description of Irr was based on regulation of *B. japonicum hemA* and *hemB* components of the heme biosynthetic pathway (24). Since *Bartonella* lacks these genes (and a mechanism for heme biosynthesis), we could not perform a direct comparison. Second, the initial "A/T-rich imperfect inverted repeat" description of the Irr *cis*-acting element was established by studying the divergently transcribed *hmuR* and *hmuT* genes, encoding a putative heme receptor and a periplasmic heme binding protein, respectively, in *B. japonicum* (44). Although *B. quintana* does contain orthologous sequences (*hutA* and *hutB*), the ORFs are not divergently transcribed, making direct comparison impossible. The ~40-bp consensus derived from all *hbp* genes (Fig. 6) is similar to this initial description (44) in that it is A/T rich, yet if a repeat exists, it would appear to be direct. Third, a less stringent Irr-associated iron control element (ICE) consensus (5′-TTTA-N_9-TAAA) (57) is found 266 times in the *B. quintana* genome, and the closest site is >1,500 bp away from the probe 3-4 overlap region (Fig. 3). Fourth, the most recently published consensus of the *B. japonicum* ICE (5′-TTTRGAA YNRTTCYAAA) (53) is not found in the probe 3-4 overlap region (with a tolerance of 3 mismatches), and the closest ClustalW alignment of ICE to the *hbpC* probe 3-4 overlap is 74 bp upstream of the EcoRV site, with 8 mismatches. Using this 8-mismatch tolerance to search the *B. quintana* genome results in 431,602 ICE sites (approximately 1 site every 3 bp). We hypothesize that either the *B. quintana* Irr *cis*-acting promoter element is distinct from that described for *B. japonicum* or the footprint size and exact nucleotide contacts therein preclude a precise consensus.

RirA, the rhizobial iron regulator, was first identified in *R. leguminosarum* (64), where derepression of iron- or heme-associated operons was ascribed to a *rirA* mutation. Further studies describe the global effect of this regulator (62, 66, 72) and show that RirA activity is highest under iron-replete conditions. A hypothetical regulatory network was proposed (63) where Irr and RirA sense the physiological consequences of extraneous iron rather than the concentration of iron, i.e., RirA is active under high-iron conditions, and Irr is active under low-iron conditions. Indeed, models of interplay between Irr, RirA, and Fur regulons have been proposed (28, 56). One noteworthy distinction is the role of Fur, depending on whether RirA is present in a particular species. In the absence of RirA (as is evident for *B. japonicum*), Fur assumes a more dominant regulatory role. Alternatively, RirA assumes the dominant iron-responsive role if present, and the function of *fur* is then downplayed (as is evident for *R. leguminosarum*). This dichotomy, although relatively unstudied, appears to exist in *Bartonella*: ORFs encoding all three of these transcription factors (Irr, Fur, and RirA) occur in *B. quintana* and *B. henselae*, yet *B. bacilliformis* does not appear to have a *rirA* gene. In accordance with these data, we demonstrate that (i) under low-hemin conditions, *rirA* transcript levels are decreased, and at high heme concentrations, an increase is apparent (Fig. 2A); (ii) *rirA* overexpression results in a significant increase in *irr* and *fur* transcript quantities, suggesting that RirA can influence the expression of these transcription factors (and in fact this is where we observed the largest average fold difference in *fur* transcript levels [Fig. 8B]); and (iii) *fur* overexpression had almost no impact on *irr* and *rirA* transcript quantities and had the least effect on the *hbp* transcript profile. Finally, this is the first analysis of *rirA* in the bartonellae, and a *rirA* overexpression strain generated a "bloodstream-like" *hbp* transcript profile. It is tempting to speculate that due to the presence of *rirA*, iron regulation in *B. quintana* and *B. henselae* (50) is like that in *R. leguminosarum*, whereas the regulation strategy of *B. bacilliformis* is predicted to be more akin to that of *B. japonicum*.

cis-acting regulatory elements related to the functions of Fur and RirA in the *Rhizobiales* have been described (21, 53, 72), but to our knowledge, such elements have not been described for any orthologue of *batR*. First, footprint analysis of the *B. japonicum irr* promoter demonstrates that *B. japonicum* Fur protects a 29-bp region (5′-AGTTGCGAGAAACTTGCATC TGCATCAT) from DNase I digestion (21). A search of the *B. quintana* genome, with a tolerance of 12, detected this sequence at 573 locations. The closest location to the *B. quintana irr* ORF is >1,600 bp upstream, and the nearest proximity to *fur*, *rirA*, *batR*, or an *hbp* is located within the *hbpB* ORF. Remarkably, of the 429 locations identified using the Fur-box as described for *E. coli* (5′-GATAATGATAATCATTATCG) (13), 19 are found within the *hbpB* ORF (with a tolerance of 6). Second, the newly proposed RirA-box (5′-TGA-N_9-TCA) (53) is found at 1,556 locations in the *B. quintana* genome, and the nearest proximity to *fur*, *rirA*, *batR*, or an *hbp* is also found within the *hbpB* ORF. It is tempting to speculate that Fur or RirA represses *hbpB*, which could explain the low quantities of *hbpB* transcripts observed throughout these studies, as well as the questionable role of HbpB in *B. quintana* (7, 41).

In this study, we used the "H-box" to search for other ORFs in the *B. quintana* genome that could potentially be regulated in the same manner as the *hbp* genes. We initially discovered the Hbp's by hemin blot analysis of *B. quintana* cellular lysates (14, 41), yet they shared no homology with other known hemin-binding proteins. Here, by studying the regulation of the *hbp* genes by using biologically relevant environmental stimuli, we have identified a *cis*-acting element that is located in the promoter regions of known heme- or iron-related ORFs (cohemolysins, heme O synthase [Fig. 7]), thereby fortifying the hypothesized function of the Hbp's in the absence of sequence-defined structural similarity. Other than the ability to bind heme (14, 17, 41, 73), the overall function of the Hbp family (or the Omp and Rop orthologues in the *Rhizobiales*) has yet to be clearly defined. "H-box" identification of a family of secreted cohemolysins is quite intriguing and, with further study, could lead to a better understanding of the function of the Hbp family, especially considering that a *B. henselae* cohemolysin orthologue causes lysis of red blood cells (32). Finally, it is tempting to speculate that heme (synthesis, acquisition, or

regulation) had a major evolutionary role in defining the niches occupied by present-day members of the *Rhizobiales*.

ACKNOWLEDGMENTS

We are grateful to Patty McIntire (UM Murdock Sequencing Facility) for providing sequence data, to Jane Koehler (UC San Francisco, San Francisco, CA) for the generous contribution of *B. quintana* strain JK31, and to Richard Birtles (University of Liverpool, Liverpool, United Kingdom) for providing *batRS* sequences before publication.

This work was supported by Public Health Service grant R01 AI053111 from the National Institutes of Health.

REFERENCES

1. **Alsmark, C. M., A. C. Frank, E. O. Karlberg, B. A. Legault, D. H. Ardell, B. Canback, A. S. Eriksson, A. K. Naslund, S. A. Handley, M. Huvet, B. La Scola, M. Holmberg, and S. G. Andersson.** 2004. The louse-borne human pathogen *Bartonella quintana* is a genomic derivative of the zoonotic agent *Bartonella henselae*. Proc. Natl. Acad. Sci. USA **101:**9716–9721.
2. **Appleby, C. A.** 1984. Leghemoglobin and *Rhizobium* respiration. Annu. Rev. Plant Physiol. Plant Mol. Biol. **35:**443–478.
3. **Applied Biosystems.** 2004. Guide to performing relative quantitation of gene expression using real-time quantitative PCR. http://docs.appliedbiosystems.com/pebiodocs/04371095.pdf.
4. **Ausubel, F., et al.** 1995. Current protocols in molecular biology. John Wiley and Sons Inc., New York, NY.
5. **Baker, H. M., B. F. Anderson, and E. N. Baker.** 2003. Dealing with iron: common structural principles in proteins that transport iron and heme. Proc. Natl. Acad. Sci. USA **100:**3579–3583.
6. **Battisti, J. M., and M. F. Minnick.** 1999. Development of a system for genetic manipulation of *Bartonella bacilliformis*. Appl. Environ. Microbiol. **65:**3441–3448.
7. **Battisti, J. M., K. N. Sappington, L. S. Smitherman, N. L. Parrow, and M. F. Minnick.** 2006. Environmental signals generate a differential and coordinated expression of the heme receptor gene family of *Bartonella quintana*. Infect. Immun. **74:**3251–3261.
8. **Birtles, R. J., T. G. Harrison, N. A. Saunders, and D. H. Molyneux.** 1995. Proposals to unify the genera *Grahamella* and *Bartonella*, with descriptions of *Bartonella talpae* comb. nov., *Bartonella peromysci* comb. nov., and three new species, *Bartonella grahamii* sp. nov., *Bartonella taylorii* sp. nov., and *Bartonella doshiae* sp. nov. Int. J. Syst. Bacteriol. **45:**1–8.
9. **Boonjakuakul, J. K., H. L. Gerns, Y. T. Chen, L. D. Hicks, M. F. Minnick, and J. E. Koehler.** 16 February 2007. Proteomic and immunoblot analysis of *Bartonella quintana* total membrane proteins identifies antigens recognized by serum from infected patients. Infect. Immun. http://iai.asm.org/cgi/content/abstract/IAI.01974-06v1.
10. **Bowden, R. A., S. M. Estein, M. S. Zygmunt, G. Dubray, and A. Cloeckaert.** 2000. Identification of protective outer membrane antigens of *Brucella ovis* by passive immunization of mice with monoclonal antibodies. Microbes Infect. **2:**481–488.
11. **Brouqui, P., and D. Raoult.** 2006. Arthropod-borne diseases in homeless. Ann. N. Y. Acad. Sci. **1078:**223–235.
12. **Buxton, P. A.** 1939. The louse: an account of the lice which infest man, their medical importance and control. Butler and Tanner, London, United Kingdom.
13. **Calderwood, S. B., and J. J. Mekalanos.** 1988. Confirmation of the Fur operator site by insertion of a synthetic oligonucleotide into an operon fusion plasmid. J. Bacteriol. **170:**1015–1017.
14. **Carroll, J. A., S. A. Coleman, L. S. Smitherman, and M. F. Minnick.** 2000. Hemin-binding surface protein from *Bartonella quintana*. Infect. Immun. **68:**6750–6757.
15. **Chevalier, G., and C. Delamarche.** 1992. Protein IIIa of *Rhizobium leguminosarum* is probably a porin. Biochimie **74:**1121–1123.
16. **Cloeckaert, A., N. Vizcaino, J. Y. Paquet, R. A. Bowden, and P. H. Elzer.** 2002. Major outer membrane proteins of *Brucella* spp.: past, present and future. Vet. Microbiol. **90:**229–247.
17. **Delpino, M. V., J. Cassataro, C. A. Fossati, F. A. Goldbaum, and P. C. Baldi.** 2006. *Brucella* outer membrane protein Omp31 is a haemin-binding protein. Microbes Infect. **8:**1203–1208.
18. **de Maagd, R. A., I. H. Mulders, H. C. Canter Cremers, and B. J. Lugtenberg.** 1992. Cloning, nucleotide sequencing, and expression in *Escherichia coli* of a *Rhizobium leguminosarum* gene encoding a symbiotically repressed outer membrane protein. J. Bacteriol. **174:**214–221.
19. **Fournier, P. E., M. F. Minnick, H. Lepidi, E. Salvo, and D. Raoult.** 2001. Experimental model of human body louse infection using green fluorescent protein-expressing *Bartonella quintana*. Infect. Immun. **69:**1876–1879.
20. **Fournier, P. E., J. B. Ndihokubwayo, J. Guidran, P. J. Kelly, and D. Raoult.** 2002. Human pathogens in body and head lice. Emerg. Infect. Dis. **8:**1515–1518.
21. **Friedman, Y. E., and M. R. O'Brian.** 2003. A novel DNA-binding site for the ferric uptake regulator (Fur) protein from *Bradyrhizobium japonicum*. J. Biol. Chem. **278:**38395–38401.
22. **Gupta, V. K., P. K. Rout, and V. S. Vihan.** 2 October 2006. Induction of immune response in mice with a DNA vaccine encoding outer membrane protein (omp31) of *Brucella melitensis* 16M. Res. Vet. Sci. doi:10.1016/j.rvsc.2006.07.014.
23. **Guzman-Verri, C., L. Manterola, A. Sola-Landa, A. Parra, A. Cloeckaert, J. Garin, J. P. Gorvel, I. Moriyon, E. Moreno, and I. Lopez-Goni.** 2002. The two-component system BvrR/BvrS essential for *Brucella abortus* virulence regulates the expression of outer membrane proteins with counterparts in members of the *Rhizobiaceae*. Proc. Natl. Acad. Sci. USA **99:**12375–12380.
24. **Hamza, I., S. Chauhan, R. Hassett, and M. R. O'Brian.** 1998. The bacterial Irr protein is required for coordination of heme biosynthesis with iron availability. J. Biol. Chem. **273:**21669–21674.
25. **Imlay, J. A.** 2002. How oxygen damages microbes: oxygen tolerance and obligate anaerobiosis. Adv. Microb. Physiol. **46:**111–153.
26. **Ito, S., and J. W. Vinson.** 1965. Fine structure of *Rickettsia quintana* cultivated in vitro and in the louse. J. Bacteriol. **89:**481–495.
27. **Jacques, I., J. M. Verger, K. Laroucau, M. Grayon, N. Vizcaino, A. Peix, F. Cortade, F. Carreras, and L. A. Guilloteau.** 2007. Immunological responses and protective efficacy against *Brucella melitensis* induced by bp26 and omp31 *B. melitensis* Rev.1 deletion mutants in sheep. Vaccine **25:**794–805.
28. **Johnston, A. W., J. D. Todd, A. R. Curson, S. Lei, N. Nikolaidou-Katsaridou, M. S. Gelfand, and D. A. Rodionov.** 20 February 2007. Living without Fur: the subtlety and complexity of iron-responsive gene regulation in the symbiotic bacterium *Rhizobium* and other alpha-proteobacteria. Biometals. http://www.rtcb.iitp.ru/PDF/17310401.pdf.
29. **Koehler, J. E.** 1996. *Bartonella* infections. Adv. Pediatr. Infect. Dis. **11:**1–27.
30. **Konkel, M. E., and K. Tilly.** 2000. Temperature-regulated expression of bacterial virulence genes. Microbes Infect. **2:**157–166.
31. **Kovach, M. E., R. W. Phillips, P. H. Elzer, R. M. Roop II, and K. M. Peterson.** 1994. pBBR1MCS: a broad-host-range cloning vector. BioTechniques **16:**800–802.
32. **Litwin, C. M., and J. M. Johnson.** 2005. Identification, cloning, and expression of the CAMP-like factor autotransporter gene (*cfa*) of *Bartonella henselae*. Infect. Immun. **73:**4205–4213.
33. **Livak, K. J., and T. D. Schmittgen.** 2001. Analysis of relative gene expression data using real-time quantitative PCR and the $2^{-\Delta\Delta}CT$ method. Methods **25:**402–408.
34. **Marsh, F., and P. A. Buxton.** 1937. Measurements of the temperature and humidity between clothes and body. J. Hyg. **37:**254–260.
35. **Martinez, M., R. A. Ugalde, and M. Almiron.** 2005. Dimeric *Brucella abortus* Irr protein controls its own expression and binds haem. Microbiology **151:**3427–3433.
36. **Martinez, M., R. A. Ugalde, and M. Almiron.** 2006. Irr regulates brucebactin and 2,3-dihydroxybenzoic acid biosynthesis, and is implicated in the oxidative stress resistance and intracellular survival of *Brucella abortus*. Microbiology **152:**2591–2598.
37. **Maurin, M., and D. Raoult.** 1996. *Bartonella* (*Rochalimaea*) *quintana* infections. Clin. Microbiol. Rev. **9:**273–292.
38. **Mekalanos, J. J.** 1992. Environmental signals controlling expression of virulence determinants in bacteria. J. Bacteriol. **174:**1–7.
39. **Mellanby, K.** 1932. The conditions of temperature and humidity of the air between the skin and shirt of man. J. Hyg. **32:**268–274.
40. **Minnick, M. F.** 2001. *Bartonella*, p. 2115–2136. *In* M. Sussman (ed.), Molecular medical microbiology. Academic Press, London, United Kingdom.
41. **Minnick, M. F., K. N. Sappington, L. S. Smitherman, S. G. Andersson, O. Karlberg, and J. A. Carroll.** 2003. Five-member gene family of *Bartonella quintana*. Infect. Immun. **71:**814–821.
42. **Myers, W. F., L. D. Cutler, and C. L. Wisseman, Jr.** 1969. Role of erythrocytes and serum in the nutrition of *Rickettsia quintana*. J. Bacteriol. **97:**663–666.
43. **Myers, W. F., J. V. Osterman, and C. L. Wisseman.** 1972. Nutritional studies of *Rickettsia quintana*: nature of the hematin requirement. J. Bacteriol. **109:**89–95.
44. **Nienaber, A., H. Hennecke, and H. M. Fischer.** 2001. Discovery of a haem uptake system in the soil bacterium *Bradyrhizobium japonicum*. Mol. Microbiol. **41:**787–800.
45. **Noya, F., A. Arias, and E. Fabiano.** 1997. Heme compounds as iron sources for nonpathogenic *Rhizobium* bacteria. J. Bacteriol. **179:**3076–3078.
46. **O'Brian, M. R.** 1996. Heme synthesis in the rhizobium-legume symbiosis: a palette for bacterial and eukaryotic pigments. J. Bacteriol. **178:**2471–2478.
47. **O'Brian, M. R., P. M. Kirshbom, and R. J. Maier.** 1987. Bacterial heme synthesis is required for expression of the leghemoglobin holoprotein but not the apoprotein in soybean root nodules. Proc. Natl. Acad. Sci. USA **84:**8390–8393.
48. **Ohl, M. E., and D. H. Spach.** 2000. *Bartonella quintana* and urban trench fever. Clin. Infect. Dis. **31:**131–135.
49. **Oliveira, M. F., J. R. Silva, M. Dansa-Petretski, W. de Souza, U. Lins, C. M. Braga, H. Masuda, and P. L. Oliveira.** 1999. Haem detoxification by an insect. Nature **400:**517–518.
50. **Park, S. Y., K. L. Kelminson, A. K. Lee, P. Zhang, R. E. Warner, D. H.**

Rehkopf, S. B. Calderwood, and J. E. Koehler. 2001. Identification, characterization, and functional analysis of a gene encoding the ferric uptake regulation protein in *Bartonella* species. J. Bacteriol. **183:**5751–5755.
51. **Qi, Z., I. Hamza, and M. R. O'Brian.** 1999. Heme is an effector molecule for iron-dependent degradation of the bacterial iron response regulator (Irr) protein. Proc. Natl. Acad. Sci. USA **96:**13056–13061.
52. **Qi, Z., and M. R. O'Brian.** 2002. Interaction between the bacterial iron response regulator and ferrochelatase mediates genetic control of heme biosynthesis. Mol. Cell **9:**155–162.
53. **Rodionov, D. A., M. S. Gelfand, J. D. Todd, A. R. Curson, and A. W. Johnston.** 15 December 2006. Computational reconstruction of iron- and manganese-responsive transcriptional networks in α-Proteobacteria. PLoS Comput. Biol. **2:**e163. doi:10.1371/journal.pcbi.0020163.
54. **Roest, H. P., C. J. Bloemendaal, C. A. Wijffelman, and B. J. Lugtenberg.** 1995. Isolation and characterization of *ropA* homologous genes from *Rhizobium leguminosarum* biovars viciae and trifolii. J. Bacteriol. **177:**4985–4991.
55. **Roest, H. P., I. H. Mulders, C. A. Wijffelman, and B. J. Lugtenberg.** 1995. Isolation of *ropB*, a gene encoding a 22-kDa *Rhizobium leguminosarum* outer membrane protein. Mol. Plant-Microbe Interact. **8:**576–583.
56. **Rudolph, G., H. Hennecke, and H. M. Fischer.** 2006. Beyond the Fur paradigm: iron-controlled gene expression in rhizobia. FEMS Microbiol. Rev. **30:**631–648.
57. **Rudolph, G., G. Semini, F. Hauser, A. Lindemann, M. Friberg, H. Hennecke, and H. M. Fischer.** 2006. The iron control element, acting in positive and negative control of iron-regulated *Bradyrhizobium japonicum* genes, is a target for the Irr protein. J. Bacteriol. **188:**733–744.
58. **Salhi, I., R. A. Boigegrain, J. Machold, C. Weise, A. Cloeckaert, and B. Rouot.** 2003. Characterization of new members of the group 3 outer membrane protein family of *Brucella* spp. Infect. Immun. **71:**4326–4332.
59. **Sander, A., S. Kretzer, W. Bredt, K. Oberle, and S. Bereswill.** 2000. Hemin-dependent growth and hemin binding of *Bartonella henselae*. FEMS Microbiol. Lett. **189:**55–59.
60. **Schwan, T. G., and B. J. Hinnebusch.** 1998. Bloodstream- versus tick-associated variants of a relapsing fever bacterium. Science **280:**1938–1940.
61. **Sola-Landa, A., J. Pizarro-Cerda, M. J. Grillo, E. Moreno, I. Moriyon, J. M. Blasco, J. P. Gorvel, and I. Lopez-Goni.** 1998. A two-component regulatory system playing a critical role in plant pathogens and endosymbionts is present in *Brucella abortus* and controls cell invasion and virulence. Mol. Microbiol. **29:**125–138.
62. **Todd, J. D., G. Sawers, and A. W. Johnston.** 2005. Proteomic analysis reveals the wide-ranging effects of the novel, iron-responsive regulator RirA in *Rhizobium leguminosarum* bv. *viciae*. Mol. Genet. Genomics **273:**197–206.
63. **Todd, J. D., G. Sawers, D. A. Rodionov, and A. W. Johnston.** 2006. The *Rhizobium leguminosarum* regulator IrrA affects the transcription of a wide range of genes in response to Fe availability. Mol. Genet. Genomics **275:**564–577.
64. **Todd, J. D., M. Wexler, G. Sawers, K. H. Yeoman, P. S. Poole, and A. W. Johnston.** 2002. RirA, an iron-responsive regulator in the symbiotic bacterium *Rhizobium leguminosarum*. Microbiology **148:**4059–4071.
65. **Vaughan, J. A., and A. F. Azad.** 1993. Patterns of erythrocyte digestion by bloodsucking insects: constraints on vector competence. J. Med. Entomol. **30:**214–216.
66. **Viguier, C., P. O. Cuív, P. Clarke, and M. O'Connell.** 2005. RirA is the iron response regulator of the rhizobactin 1021 biosynthesis and transport genes in *Sinorhizobium meliloti* 2011. FEMS Microbiol. Lett. **246:**235–242.
67. **Vinson, J.** 1966. In vitro cultivation of the rickettsia agent of trench fever. Bull. W. H. O. **35:**155–164.
68. **Vizcaino, N., P. Caro-Hernandez, A. Cloeckaert, and L. Fernandez-Lago.** 2004. DNA polymorphism in the omp25/omp31 family of *Brucella* spp.: identification of a 1.7-kb inversion in *Brucella cetaceae* and of a 15.1-kb genomic island, absent from *Brucella ovis*, related to the synthesis of smooth lipopolysaccharide. Microbes Infect. **6:**821–834.
69. **Wexler, M., J. D. Todd, O. Kolade, D. Bellini, A. M. Hemmings, G. Sawers, and A. W. Johnston.** 2003. Fur is not the global regulator of iron uptake genes in *Rhizobium leguminosarum*. Microbiology **149:**1357–1365.
70. **Yang, J., H. R. Panek, and M. R. O'Brian.** 2006. Oxidative stress promotes degradation of the Irr protein to regulate haem biosynthesis in *Bradyrhizobium japonicum*. Mol. Microbiol. **60:**209–218.
71. **Yang, J., I. Sangwan, A. Lindemann, F. Hauser, H. Hennecke, H. M. Fischer, and M. R. O'Brian.** 2006. *Bradyrhizobium japonicum* senses iron through the status of haem to regulate iron homeostasis and metabolism. Mol. Microbiol. **60:**427–437.
72. **Yeoman, K. H., A. R. Curson, J. D. Todd, G. Sawers, and A. W. Johnston.** 2004. Evidence that the *Rhizobium* regulatory protein RirA binds to *cis*-acting iron-responsive operators (IROs) at promoters of some Fe-regulated genes. Microbiology **150:**4065–4074.
73. **Zimmermann, R., V. A. Kempf, E. Schiltz, K. Oberle, and A. Sander.** 2003. Hemin binding, functional expression, and complementation analysis of Pap 31 from *Bartonella henselae*. J. Bacteriol. **185:**1739–1744.

Editor: F. C. Fang